

Electrical Properties of Semiconducting CdF₂:Y

R. P. KHOSLA

Research Laboratories, Eastman Kodak Company, Rochester, New York 14650

(Received 3 February 1969)

Measurements of resistivity and the Hall coefficient in the temperature range 425–4.2°K have been made on single crystals of semiconducting CdF₂ doped with yttrium (Y). The Y concentrations ranged from 0.002–1 mole %. The characteristic behavior of impurity-band conduction is observed, with the activation energies ϵ_1 , ϵ_2 , and ϵ_3 . The onset of impurity-band conduction occurs at higher temperatures than in other semiconductors. No degeneracy effects are seen for the highest concentrations observed. The data are analyzed on the basis of simple semiconductor theory, assuming a hydrogenic nature of the Y donor. Using the value of effective polaron mass $m_p \approx 0.9m_e$ and the static dielectric constant $\epsilon_0 = 8.1$, we find that the calculated ionization energy is larger than the experimental value. The impurity-banding behavior cannot be characterized in a fashion similar to what has been done in other semiconductors. Alternative analyses are suggested. The Hall coefficient is analyzed on the basis of the two-band model: the conduction band and the impurity band. At temperatures above 250°K, the Hall-mobility data can be fitted by assuming polar optical mode and an acoustic mode as the dominant scattering mechanisms. The deformation potential was found to be 8.2 ± 1 eV. Below 250°K, ionized impurity-scattering is the additional mechanism. At temperatures below $\sim 80^\circ\text{K}$, the mobility falls off sharply owing to impurity banding.

I. INTRODUCTION

PURE crystals of CdF₂ are highly insulating. The material can be made semiconducting by doping with various trivalent-metal ions (especially the rare earths) and annealing in cadmium-metal vapor at relatively low temperatures. Weller¹ has discussed the variety of dopants that would result in a semiconductor, as well as those that would not. The process of conversion of insulating CdF₂ to a semiconducting state by cadmium-metal annealing is outlined by Kingsley and Prener.^{2,3} A survey of the work on CdF₂ is given by Eisenberger and Pershan.⁴ The electrical properties were, in general, measured down to liquid-nitrogen temperature.

CdF₂ has a large band gap $E_G = 6.0$ eV. It can be made only *n* type. Khosla and Matz⁵ have reported, from their Hall-coefficient and thermoelectric-power measurements, an effective polaron mass $m_p \approx 0.9m_e$, a bare conduction mass $m_e \approx 0.45m_e$, and a coupling constant $\alpha \approx 3.3$; whereas Eisenberger *et al.*⁶ have reported a value of $m_p = 11m_e$ on the basis of cyclotron resonance measurements. The transport measurements of Khosla and Matz were made on carriers in thermal equilibrium with the lattice vibrations at high temperatures, whereas Eisenberger *et al.* used photoexcited carriers at very low temperatures, where the impurity-banding effects are predominant. It is possible that these carriers may not be in the conduction-band states. It may also be pointed out that the cyclotron measurements were done at only one frequency ≈ 12.73 Gc/sec. Though the discrepancy cannot be resolved as yet, we will use the

values reported by Khosla and Matz for our analysis as these explain our Hall-coefficient, mobility, and thermoelectric-power data in a self-consistent manner.

We have investigated the electrical properties—resistivity, Hall coefficient, and mobility—of semiconducting CdF₂:Y over the temperature range 425–4.2°K. The measurements at very high temperatures are limited by the annealing temperatures, as the semiconducting samples convert to the insulating state. The difficulties encountered by other workers^{1,7} in making measurements down to very low temperatures have been overcome as will be discussed in Sec. II. Resistivity and Hall-coefficient data were obtained between 425 and 4.2°K, and between 425 and 30°K, respectively, for most of the samples.

Measurements were made on samples with room-temperature carrier concentrations as high as 6.7×10^{18} cm⁻³. We note that changing the annealing temperature, for a fixed amount of dopant, does give rise to varying carrier concentration at room temperature.⁷ Impurity-banding effects are similar to those seen in other semiconductors.^{8,9} The Hall data are analyzed on the basis of conduction in the two bands¹⁰: the conduction band and the impurity band. Estimates of the mobility ratio b in the conduction band to that in the impurity band are made. The exponential behavior of mobility in the impurity-band conduction regime is understandable in terms of the exponential dependence of the ratio of the carriers in the conduction band to that in the impurity band. In the temperature range 250–425°K, the Hall-mobility data for our lightly

¹ P. F. Weller, *Inorg. Chem.* **4**, 1545 (1965).

² J. D. Kingsley and J. S. Prener, *Phys. Rev. Letters* **8**, 315 (1962).

³ J. S. Prener and J. D. Kingsley, *J. Chem. Phys.* **38**, 667 (1963).

⁴ P. Eisenberger and P. S. Pershan, *Phys. Rev.* **167**, 292 (1968).

⁵ R. P. Khosla and D. Matz, *Solid State Commun.* **6**, 859 (1968).

⁶ P. Eisenberger, P. S. Pershan, and D. R. Bosomworth, *Phys. Rev. Letters* **21**, 543 (1968).

⁷ J. S. Prener and H. H. Woodbury, in *Proceedings of the Seventh International Conference on the Physics of Semiconductors, Paris, 1964* (Academic Press Inc., New York, 1964), p. 1231.

⁸ H. Fritzsche, *J. Phys. Chem. Solids* **6**, 69 (1958). See a list of references for impurity-banding effects in other materials in Ref. 2 of H. Fritzsche and M. Cuevas, *Phys. Rev.* **119**, 1238 (1962).

⁹ H. Fritzsche, *Phys. Rev.* **99**, 406 (1955).

¹⁰ C. S. Hung, *Phys. Rev.* **79**, 727 (1950).

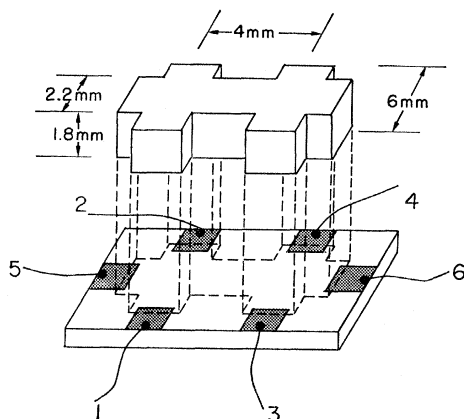


Fig. 1. Spider-shaped sample, and the glass plate with evaporated contacts used as a mount. In-Ga alloy was used as the solder.

doped $\text{CdF}_2:\text{Y}$ samples and those of Prener and Woodbury⁷ for $\text{CdF}_2:\text{Yb}$ samples can be represented either by an exponential or a power law of temperature as is discussed in Sec. IV. Similar difficulties have been experienced in other polar semiconductors,¹¹ and it is difficult to decide between the two behaviors. The exponential behavior suggests polar optical mode scattering¹² as the dominant scattering, while the power dependence ($\mu\alpha T^n$, where n varies from -1.2 to -1.4) suggests that acoustic mode scattering¹³ is the dominant mechanism. However, neither of these mechanisms independently fits the experimental mobility at high temperatures, but the combination of them gives a fit down to 250°K . Between 250 and 80°K , ionized impurity scattering¹⁴ is the additional scattering mechanism. At temperatures lower than 80°K , impurity-band effects are dominant.

II. EXPERIMENTAL DETAILS

Single crystals of CdF_2 doped with yttrium (0.002–1 mole %) were grown by the Bridgman technique.¹⁵ These samples were annealed in Cd metal at various temperatures ranging from 200 to 500°C . Samples were cut in the form of spiders (see Fig. 1) with an ultrasonic cutter. They had dimensions of $10 \times 2.2 \times 1.8$ mm.³ The samples were lapped by using various grit sizes of Al_2O_3 on flannel cloth, after which, they were etched with concentrated HCl for 5–10 sec. They were then washed in alcohol several times. Since CdF_2 is hygroscopic, no water was used after etching.

A variety of techniques for making electrical contacts were tried, including those used by previous workers.^{1,7}

¹¹ H. P. R. Frederikse and W. R. Hosler, *Phys. Rev.* **161**, 822 (1967); R. L. Petritz and W. W. Scanlon, *ibid.* **97**, 1620 (1955).

¹² D. C. Langreth, *Phys. Rev.* **159**, 717 (1967).

¹³ W. Shockley, *Electrons and Holes in Semiconductors* (D. Van Nostrand Co., Inc., New York, 1950), Chap. 11.

¹⁴ H. Brooks, *Advances in Electron Physics* (Academic Press Inc., New York, 1955), Vol. 7, p. 156.

¹⁵ F. Trautweiler, F. Moser, and R. P. Khosla, *J. Phys. Chem. Solids* **29**, 1869 (1968).

The following are the two most dependable methods, giving Ohmic and noise-free contacts down to very low temperatures.

(a) The Cerroseeal 35-mercury amalgam was used to paint the places on the sample where the contacts were to be made. The sample was heated with a heat gun (blower), and a thin rod of Cerroseeal solder was melted on the painted spots. On cooling, it formed mechanically strong Ohmic contacts. Electrical leads were soldered to these contacts with Cerroseeal solder.

(b) An In-Ga (50-50) alloy, which is a liquid paste at room temperature, was used. Six contacts were evaporated on glass plates as shown in Fig. 1 using first titanium and then gold (approximately 1000 \AA thick). The arrangement of the contacts was such that our spider-shaped samples could be placed with all the arms fitted onto the evaporated contacts. Lead wires were soldered as shown with a Pb-Sn solder. The sample was then placed in position. To provide good contacts, the arms and the evaporated contacts were wetted together with In-Ga alloy.

The leads 5 and 6 were used for current. The resistivity of the sample was determined by measuring the potential difference between contacts 1 and 3, or between 2 and 4. The Hall potential was measured between either contacts 1 and 2 or 3 and 4. Five contacts to the crystal were used at any one time. However, the sixth contact was used from time to time during the course of the experiment to check the homogeneity of the sample by measuring a second set of resistivity and Hall potentials. The sample holder was mounted in an Andonian Dewar in which the temperature could be varied continuously between 4.2 and $\sim 360^\circ\text{K}$. High-temperature data up to 425°K were taken by immersing the samples in a silicone oil bath. A 6-in. Varian magnet provided the necessary magnetic field.

All external wiring in the measuring circuit was RG-58/U cable with Teflon connectors to minimize leakage. The voltage to the sample was applied by a battery and the current through the sample was read on a Keithley 601 electrometer. The 610B electrometer was used to read the potential difference across the leads 1 and 3 or 2 and 4. The current contacts were kept floating. Hall voltage was read on a Keithley 150B microvoltmeter, nanoammeter. A nanovolt source was used to buck out any offset voltage on the Hall leads. At lower temperature, where difficulties due to noise were encountered and the Hall voltage was a few microvolts, the output of the 150B was put on a recorder and integrated. Two directions of current and the two directions of the magnetic field were used to avoid any spurious effects.

III. RESULTS

A. Resistivity and Hall Coefficient

The electrical measurements have been made to much lower temperatures than have been previously

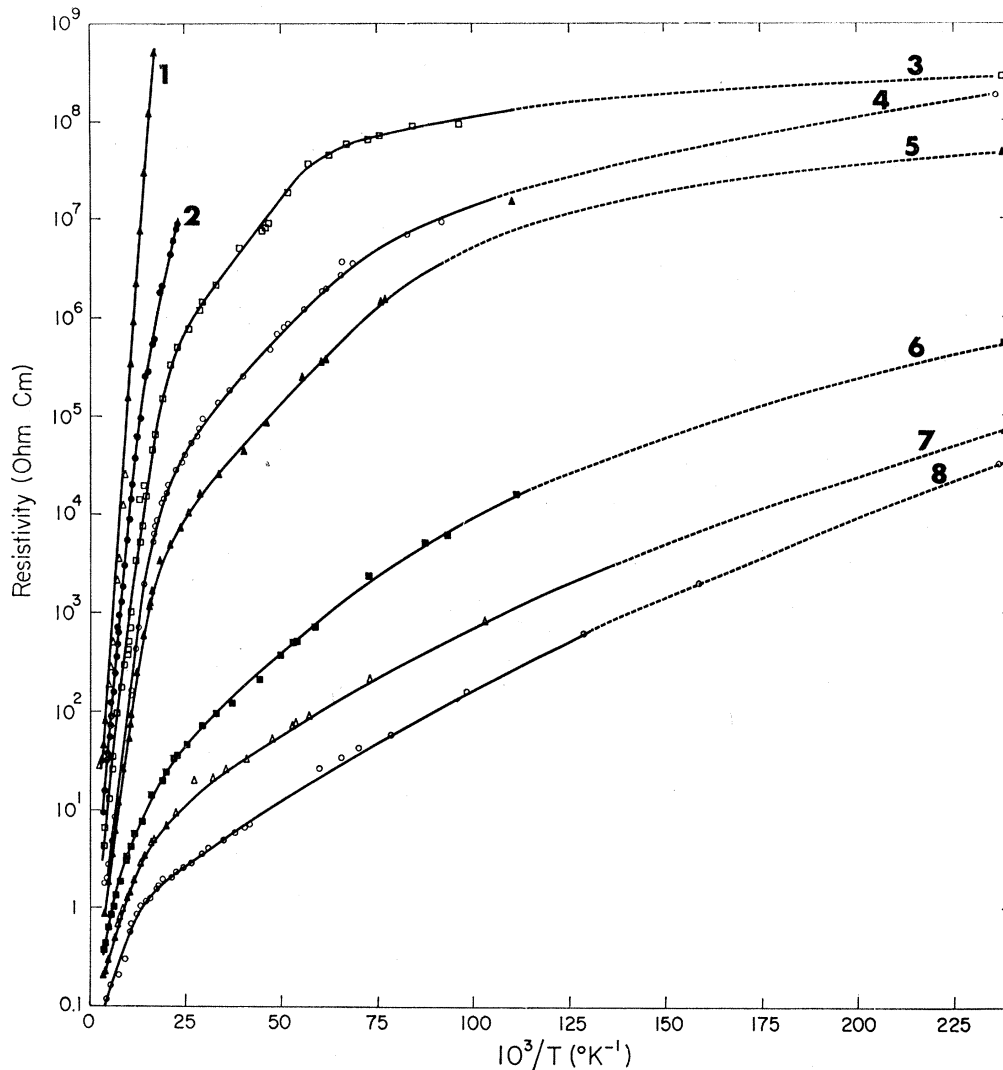


FIG. 2. Resistivity versus $10^3/T$ for various samples. Sample numbers are identified in Table I.

reported.^{1,7} Resistivity could be measured on most crystals down to 4.2°K. However, the Hall voltage was difficult to measure below 40°K, because of the small signals and noisy contacts.

In Fig. 2, we plot the resistivity ρ of various samples versus $10^3/T$ over a large temperature range. Figure 3 shows the measured Hall coefficient R_H versus $10^3/T$. Although the data were taken for a large number of samples, only representative data are plotted for the sake of clarity. Previous workers,^{1,7} who made their measurements down to liquid-nitrogen temperature in CdF_2 containing Yb and other dopants, had suggested the existence of impurity banding because of the beginning of the maxima in the Hall coefficient in R_H versus $10^3/T$ plots. Our measurements down to low temperatures also strongly suggest the existence of impurity banding.

Samples with as high a room-temperature carrier concentration as $6.7 \times 10^{18} \text{ cm}^{-3}$ have been measured, but we do not see any degeneracy. However, three carrier concentration ranges can be distinguished as follows:

(i) Two activation energies exist, which for samples with room-temperature carrier concentration $> 1.8 \times 10^{18} \text{ cm}^{-3}$ are characterized as ϵ_1 and ϵ_3 in the usual fashion^{8,9} (samples 7 and 8). The Hall coefficient of these samples has a broad maximum.

(ii) In samples with lower room-temperature carrier concentration, $< 1.8 \times 10^{18} \text{ cm}^{-3}$, we see the onset of an intermediate activation energy, designated as ϵ_2 . As the room-temperature carrier concentration of the samples decreases, the temperature range for which this intermediate region exists increases; with further decrease in room-temperature carrier concentration of

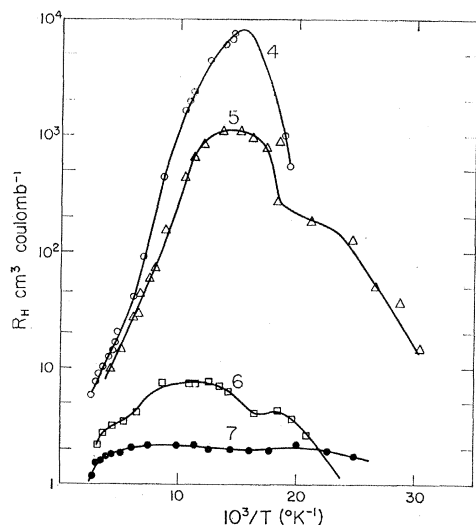


FIG. 3. Hall coefficient versus $10^3/T$ for some of the samples of Fig. 2.

samples, the temperature range for this ϵ_2 region decreases and finally vanishes (samples 3–6).

(iii) After the vanishing of the ϵ_2 region, we find a region $< 5 \times 10^{17} \text{ cm}^{-3}$ which looks similar to region (i) but with higher values of ϵ_1 . As the room-temperature carrier concentration of the samples decreases further, the resistivity of the samples increases very rapidly. We are unable to determine the ϵ_3 region in these high resistivity samples (samples 1 and 2).

Table I lists the values of the carrier concentrations, Hall coefficient, resistivity, and mobility, at room temperature, of various samples. In Table II, the activation energies for some samples, as obtained from $\ln \rho$ versus $10^3/T$ plots (and using the expression $\rho = A_1 e^{\epsilon_1/kT} + A_2 e^{\epsilon_2/kT} + A_3 e^{\epsilon_3/kT}$, are given. Tables I and II show that, for samples 2–5, although the amount of Y dopant was the same (0.01 mole %), their characteristics vary. The annealing temperature in these samples was not measured. We measured the resistivity ρ and

TABLE I. Resistivity, Hall coefficient, and mobility at 300°K of various Y-doped CdF₂ crystals.

Sample No.	Amount of yttrium (mole %)	T_{anneal} (°C)	$\rho_{300^\circ\text{K}}$ ($\Omega \text{ cm}$)	$R_{H300^\circ\text{K}}$ ($\text{cm}^3 \text{ C}^{-1}$)	$\mu_{300^\circ\text{K}}$ ($\text{cm}^2 \text{ V}^{-1} \text{ sec}^{-1}$)
1	0.002	~500	35.0	216.0	6.2
2	0.01	a	7.8	45.0	5.8
3	0.01	a	2.0	12.5	6.0
4	0.01	a	1.41	9.15	6.5
5	0.01	a	0.69	9.6	13.8
6	1.0	~500	0.36	2.2	6.2
7	0.1	~500	0.18	1.53	8.7
8	0.1	500	0.096	0.94	9.8
9	0.1	200	0.74	5.31	7.2
10	0.01	500	0.25	4.0	16.2
11	0.01	200	0.71	9.56	13.5

* Annealing temperature is not accurately known.

TABLE II. Values of activation energies determined from resistivity versus $10^3/T$ plots.

Sample No.	$n_{300^\circ\text{K}}$ (10^{16} cm^{-3})	ϵ_1 (10^{-3} eV)	ϵ_2 (10^{-3} eV)	ϵ_3 (10^{-3} eV)
1	2.9	100.2
2	14.0	89.4
3	50.0	80.8	9.9	0.15
5	65.0	60.6	8.2	0.98
4	67.0	62.4	8.8	1.70
11	76.0	80.0	7.6	1.83
9	120.0	42.8	8.4	2.32
10	180.0	61.2	7.4	2.60
6	310.0	50.3	6.9	2.30
7	410.0	27.8	...	2.60
8	670.0	22.1	...	3.10

Hall coefficient R_H at room temperature of another set of 0.01 mole % Y samples annealed at precisely controlled temperatures. It was found that $\rho_{300^\circ\text{K}}$ and $R_{H300^\circ\text{K}}$ were the same for samples annealed at 400 and 500°C but, $\rho_{300^\circ\text{K}}$ increased and $R_{H300^\circ\text{K}}$ decreased as the annealing temperature decreased. Thus the variations in the characteristics of samples 2–5 (even though they had the same Y dopant, 0.01 mole %) can be attributed to varying annealing temperature. At the same time, this experimental check indicated that the insulating CdF₂ converts to the semiconducting state at temperatures between 400 and 500°C. This finding is supported by the observations of Prener and Kingsley³ who found that cadmium-annealed crystals at 500°C could be returned to their original insulating state by heating in vacuum at temperatures above 400°C.

For the sake of analysis and characterization of CdF₂, four samples, numbered 8–11, with 0.01 and

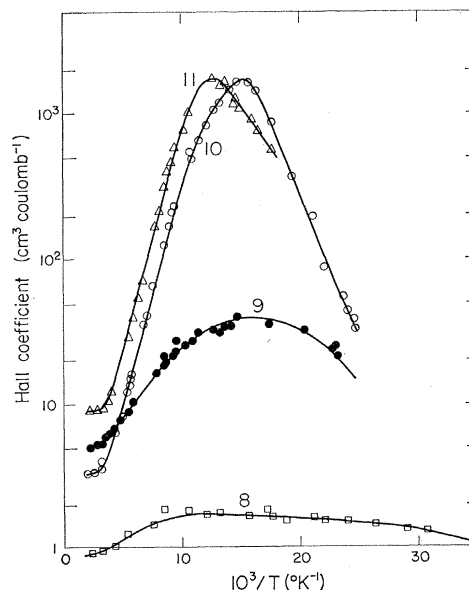


FIG. 4. Hall coefficient versus $10^3/T$ of 0.01 mole % and 0.1 mole % Y samples, cadmium annealed at 500 and 200°C, respectively. Sample numbers are identified in Table I.

0.1 mole % Y were annealed under precisely controlled temperatures of 500 and 200°C, respectively. Hall coefficient and mobility μ versus $10^3/T$ for these samples are plotted in Figs. 4 and 5, respectively.

B. Atomic Absorption Analysis

Table III gives the results of atomic absorption analysis for yttrium. The discrepancy between the measured and nominal values is within the experimental error of $\sim 10\%$ of the atomic absorption analysis. Thus for the interpretation of our data, we will assume that the number of donors N_D is equal to the nominal value of the Y dopant introduced.

IV. ANALYSIS AND DISCUSSION

Figure 4 shows that when the annealing temperature is lowered, the Hall coefficient increases or there is a decrease in the number of electrons. This is understandable from the way Cd annealing converts insulating CdF_2 to semiconducting CdF_2 .^{2,3} One would expect, therefore, to obtain quite a wide range of free electron concentration by varying the annealing temperatures. The carrier concentration ranges might overlap for two different amounts of dopants. For example, in Fig. 4, sample 10 has a higher carrier concentration than sample 9 at room temperature, even though the former had only 0.01 mole % Y and the latter 0.1 mole % Y. Sample 10, however, was annealed at 500°C, whereas sample 9 was annealed at only 200°C.

A. Impurity Banding

We find from Table II, that as the room-temperature carrier concentration decreases, ϵ_1 increases, whereas ϵ_3 decreases, but ϵ_2 remains substantially constant. In *n*-Ge,⁸ ϵ_1 and ϵ_3 have a similar concentration dependence, but ϵ_2 decreases as carrier concentration increases, in contrast to the almost constant values of ϵ_2 in CdF_2 . In *p*-Ge samples⁹ with the ϵ_2 regime in the intermediate concentration range, it was seen that the Hall coefficient exhibited two distinct maxima, whereas *n*-Ge samples⁸ having the ϵ_2 region did not exhibit the two maxima distinctly. In CdF_2 , we note only two maxima for samples 5 and 6, but such behavior is not apparent for samples 3, 4, and 9–11, which also exhibit an intermediate concentration regime. Either the temperature range for which the ϵ_2 region exists is rather broad, or polaron effects are influential in determining the impurity-banding behavior in ionic crystals.

For quantitative analysis, we assume the hydrogenic nature of the Y donor. The ionization energy is calculated by using the expression $\epsilon_i = 13.6m^*/\epsilon_0^2$ and the effective-Bohr radius a^* , given by the expression $a^* = \epsilon_0/m^*$ (0.53 Å), where ϵ_0 is the static dielectric constant and is equal to 8.1,¹⁶ and m^* is the effective mass. We wish to compare the calculated ϵ_i with the

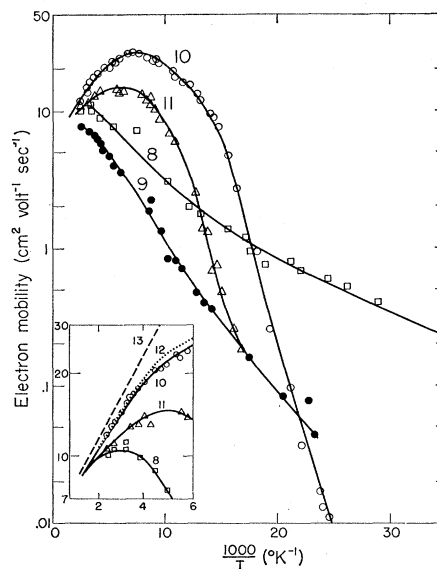


FIG. 5. Mobility versus $10^3/T$ for samples of Fig. 4. Inset is drawn to show that the experimental mobility can be extrapolated to converge at high temperatures. Samples 12 and 13 are $\text{CdF}_2: 0.01\% \text{ Yb}$ and $\text{CdF}_2: 0.002\% \text{ Yb}$, respectively, of Ref. 7.

experimental value, and also to compare the average interdonor distance $d = (3/4\pi N_D)^{1/3}$ with a^* (N_D = number of donors). If $d < 2a^*$, then the samples should show degeneracy. If $2a^* < d < 5a^*$, the samples are in the intermediate concentration region having activation energies ϵ_1 , ϵ_2 , and ϵ_3 . If $d > 5a^*$, the samples are in the pure region having activation energies ϵ_1 and ϵ_3 .¹⁷ In Table IV, we give the values of d for various amounts of dopants, and we consider four cases involving different choices of ϵ and m^* .

Case 1. In column 3, Table IV, we give the values of d/a^* , where a^* is calculated using the value of $m^* \cong 0.9m_e$.⁴ From this we find that only sample 6, with 1.0 mole % Y, falls within the criterion $2a^* < d < 5a^*$ in conformity with the observed three activation energies. For all other dopants $d > 5a^*$, even though samples 3, 4, 5, and 9–11, according to Table II, lie in the intermediate concentration range. Furthermore, using the above value of m^* , we find an ionization

TABLE III. Comparison of the atomic absorption analysis with the nominal value of yttrium dopant.

Ingot No.	Amount of yttrium		Atomic absorption (wt %)	Number of donors N_D (cm^{-3})
	Nominal (mole %)	(wt %)		
B-21	1.0	0.56	$\begin{cases} 0.36 \\ 0.38 \end{cases}$	1.66×10^{20}
B-23	0.1	0.056	0.054	2.56×10^{19}
B-12	0.01	0.0056	0.0053	2.56×10^{18}
B-22	0.01	0.0056	$\begin{cases} 0.0033 \\ 0.0039 \end{cases}$	1.65×10^{18}
B-24	0.002	0.0012	<0.001	$<4.25 \times 10^{17}$

¹⁶ D. R. Bosomworth, Phys. Rev. **157**, 709 (1967).

¹⁷ N. F. Mott and W. D. Twose, Advan. Phys. **10**, 107 (1961).

TABLE IV. Average interdonor distance \bar{d} in comparison with the effective Bohr radius a^* .

Amount of Y dopant (mole %)	\bar{d} (Å)	\bar{d}/a^*			
		$\epsilon_0=8.1$ $m^*=0.9m_e$	$\epsilon_0=4.6$ $m^*\approx 0.45m_e$	$\epsilon_0=4.6$ $m^*\approx 0.15m_e$	$\epsilon_0=8.1$ $m^*\approx 0.45m_e$
1.0	11.3	2.40	2.04	0.68	1.20
0.1	21.1	4.44	3.77	1.24	2.22
0.01	45.5	9.55	8.13	2.73	4.78
0.002	77.7	16.3	15.46	4.70	8.15

energy of the hydrogenic levels equal to 0.18 eV. This value is much larger than the measured value ϵ_1 (see Table II), even for our most lightly doped samples.

Case 2. The use of the effective density-of-states polaron mass m_p for m^* and the static dielectric constant for the above calculations is questionable. The material being highly polar,⁴ we cannot neglect the use of the dynamic dielectric constant. The wave functions for the electrons at the donor sites may be better described if the value of m_e is used for m^* to calculate a^* and ϵ_i . Kubo¹⁸ has treated the problem of a hydrogenic donor state in polar crystals, where he takes into account the possibility that the lattice cannot follow the electron. He shows that ϵ_i can still be calculated with the expression $\epsilon_i=13.6m^*/\epsilon_0^2$, but the static dielectric constant must be replaced by an effective dielectric constant ϵ^* , given by the expression

$$1/\epsilon^* = 1/\epsilon_0 + \frac{5}{16}(1/\epsilon_\infty - 1/\epsilon_0).$$

Substituting the appropriate values, $\epsilon_0=8.1$ and $\epsilon_\infty(=2.4)$,¹⁷ one obtains $\epsilon^*=4.6$. We use this value of ϵ^* and that of the bare conduction mass $m_c\approx 0.45m_e$ to calculate a^* and ϵ_i , which gives $\epsilon_i\approx 0.28$ eV, which is very much larger than the value of ionization energies obtained experimentally. Also, the values of \bar{d}/a^* (see column 4, Table IV) give the same discrepancies with respect to the observed activation energies for various amounts of Y dopants, as found in case 1.

Case 3. If we were to obtain a calculated value of ϵ_i , using ϵ^* (as above), consistent with the experimental value, we would find that $m^*\approx 0.15m_e$. This value is much smaller than the values calculated by us earlier.⁵ It is, in fact, too small to explain in a self-consistent manner our experimental values of Hall coefficient, thermoelectric power, and mobility. Furthermore, when \bar{d} is compared to a^* (see column 5, Table IV), only samples 3-5, 10, and 11, with 0.01 mole % Y, are in the intermediate concentration regime as observed experimentally. But samples 6-9, which are expected to show degeneracy, do not show such a behavior.

Case 4. We find that by using the value of ϵ_0 and the mass $m^*=m_e$, the value of ϵ_i is calculated to be 0.09 eV and $a^*=9.4$ Å. This value of ϵ_i is in good agreement with the experimental value of some of our lightly doped samples (see Table II). In Table IV, column 6, we give the values of \bar{d}/a^* . Samples 3-5, 10, and 11,

with 0.01 mole % Y, and 9 with 0.1 mole % Y, and Cd annealed at 200°C, which show the ϵ_2 region, are now within the $2a^*<\bar{d}<5a^*$ criterion. But sample 2, even though it has 0.01 mole % Y, is not in this region. As we have argued in Sec. III, the annealing temperature for sample 2 is very low. When the annealing temperature is low ($<500^\circ$), all the Y donors are not uncompensated, suggesting large compensation. At the same time, sample 6, with 1.0 mole % Y, and samples 7 and 8, with 0.1 mole % Y, should show degeneracy and the intermediate regime, respectively. This we do not see. We suggest that, for very heavily doped samples, all the donors are not fully uncompensated at 500°C, resulting in incomplete conversion of insulating CdF₂ to the semiconducting state, and a large compensation. From this, we infer that if complete conversion does not take place, then the large compensation by the interstitial F^- and other compensators increase the resistivity, as has indeed been seen by Fritzsche,⁸ and mask the true characteristics of these samples.

Analysis in case 4 above, however, neglects any polaron effects, which is not understandable, since the material is polar with a coupling constant $\alpha\approx 3.3$. The lack of good agreement between theory and experiment suggests that the simple semiconductor theories do not adequately describe the donor states in a polar material.

B. Two-Band Conduction

We have analyzed the Hall-coefficient data of samples 8-10 using a two-band model,¹⁰ in which the conductivity and the Hall coefficient are given by

$$\sigma = \sigma_1 + \sigma_2 \quad (1)$$

and

$$R_H = (R_1\sigma_1 + R_2\sigma_2)/(\sigma_1 + \sigma_2)^2, \quad (2)$$

where R_1 and σ_1 are the Hall coefficient and conductivity of carriers in the conduction band and R_2 and σ_2 are the Hall coefficient and conductivity of carriers in the impurity band. Assuming that the Hall mobility = drift mobility, Eqs. (1) and (2) can be rewritten as

$$n_e\mu = n_1e\mu_1 + n_2e\mu_2 \quad (3)$$

and

$$R_H = (n_1e\mu_1^2 + n_2e\mu_2^2)/(n_1e\mu_1 + n_2e\mu_2)^2, \quad (4)$$

where

$$R_1 = 1/n_1e, \quad \sigma_1 = n_1e\mu_1;$$

$$R_2 = 1/n_2e, \quad \sigma_2 = n_2e\mu_2,$$

¹⁸ R. J. Kubo, J. Phys. Soc. Japan **3**, 254 (1948).

n_1 and μ_1 are the electron concentration and the mobility in the conduction band, and n_2 and μ_2 are the electron concentration and the mobility in the impurity band. Introducing $b = \mu_1/\mu_2$, $n_1/n_0 = x$, and $n_2/n_0 = 1 - x$ (where n_0 is the exhaustion-carrier concentration), one can obtain¹⁹ from Eqs. (3) and (4) an expression for mobility:

$$\mu = [\mu_1/b(n_1b^2 + n_2)] / (n_1b + n_2) \quad (5)$$

and an expression for Hall coefficient

$$R_H = [xb^2 + (1-x)] / n_0e[xb + (1-x)]^2. \quad (6)$$

We can also obtain an expression for b in terms of R_H maximum and R_H exhaustion by introducing the equality

$$n_1e\mu_1 = n_2e\mu_2 \quad (7)$$

at the Hall-coefficient maxima in the R_H versus $10^3/T$ plot. In Eq. (7), it is assumed μ_1 and μ_2 are independent of temperature. The expression for b is given by

$$(R_H)_{\max} / (R_H)_{\text{exh}} = (b+1)^2 / 4b. \quad (8)$$

Using expressions (6) and (8), one can calculate b . We can also obtain the value of n_1 and n_2 , or R_{H1} and R_{H2} at any temperature. The calculated values of b , the mobility ratio in the two bands, are given in Table V. In Eq. (5), we find that when $n_2 \ll n_1$, then $\mu = \mu_1$, which is to be expected, when most of the carriers are in the conduction band; when $n_2 \gg n_1$, then $\mu = \mu_1/b = \mu_2$, or the total mobility is the mobility due to conduction in the impurity band.

In an intermediate situation, when a large number of the carriers are in the impurity band, but a good fraction of them are still in the conduction band, i.e., when $n_2 > n_1b_1$ but less than n_1b^2 , then

$$\mu = \mu_1b(n_1/n_2). \quad (9)$$

We note from Fig. 5 that the value of μ decreases as the temperature decreases. This decrease corresponds to the decrease of n_1/n_2 . We know that the depletion of n_1 or the occupancy of donors in the impurity band with respect to temperature takes place exponentially with a certain activation energy ϵ . Therefore, we attribute the exponential decrease of μ with temperature to the exponential decrease of n_1/n_2 .

C. Mobility

We shall now discuss the mobility of these samples at relatively higher temperatures in terms of the scattering mechanisms involved. As pointed out earlier (Sec. I), in the temperature range 250–425°K, the mobility data can be represented by an exponential as well as a power law of temperature. The data seem to be converging at higher temperatures, > 700°K, for our samples and those of Prener and Woodbury⁷ (see Figs. 5 and 6), when extrapolated. (The measurements to

TABLE V. Exhaustion-carrier concentration n_0 , the number of the acceptors N_A , the compensation ratio K , and the calculated values of mobility ratio b for samples 8–11.

Sample No.	N_D (10^{17} cm^{-3})	n_0 (10^{17} cm^{-3})	N_A (10^{17} cm^{-3})	$K = N_A/N_D$	$b = \mu_1/\mu_2$
8	256.0	67.0	189.0	0.74	4.2
9	256.0	12.1	243.9	0.95	25.5
10	25.6	18.6	7.0	0.27	2022.0
11	25.6	6.61	18.99	0.74	718.0

such high temperatures are unfortunately not possible, as the sample returns to the insulating state.³) This shows that at higher temperatures μ depends on the intrinsic parameters of the material, rather than the amount and type of dopant.

a. Polar Optical Mode Scattering

It has been assumed in the literature that the polar optical scattering limits the mobility at higher temperatures.⁴ Langreth¹² gives an expression for mobility for the intermediate coupling region $\alpha \approx 3$ which is valid in the temperature range of our measurements. This expression is

$$\mu_p = (e\hbar/2\alpha m_p b \theta) [1 + 1.53(T/\theta)] (e^{\theta/T} - 1), \quad (10)$$

where α is the polar optical-phonon coupling constant ≈ 3.3 , m_p the polaron mass $\approx 0.9m_e$, and θ the Debye temperature¹⁵ = 550°K. The calculated value of $\mu_p \approx 45 \text{ cm}^2/\text{V sec}$ at room temperature. This is about three times the value of μ_{exp} for our samples. One wonders, however, if Langreth's theory is applicable, since in his

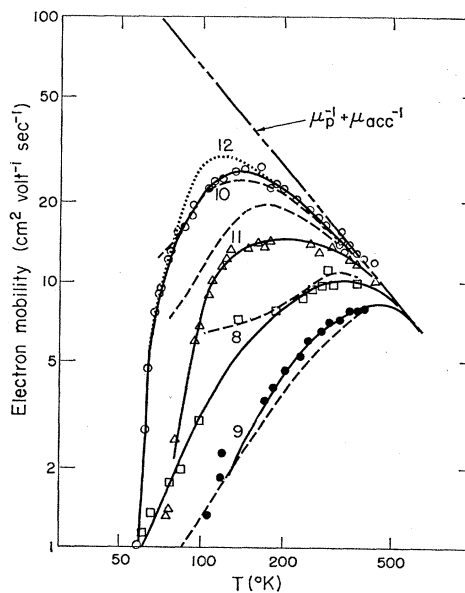


Fig. 6. Mobility versus temperature for the samples in Fig. 5. Figure is drawn for comparison with the calculated mobility due to various mechanisms. All open points are experimental, and $\mu_p^{-1} + \mu_{\text{acc}}^{-1}$ is as indicated. The dashed lines give the value of μ_{Tot}^{-1} as in Eq. (14) of the text and the dotted points (No. 12) represent the CdF₂:0.01% Yb sample of Ref. 7.

¹⁹ R. J. Sladek, J. Phys. Chem. Solids 5, 157 (1958).

theory it is assumed that the major contribution to scattering arises only from resonant phonon absorption, i.e., real phonon emission is not considered. If real phonon emission is significant, this may reduce the μ_p and allow for a negative value of the parameter S ($\tau\alpha E^S$; earlier Khosla and Matz⁴ showed that to make the results of the Hall coefficient and thermoelectric power self-consistent, it was necessary to have an effective mass value of $0.9 m_e$ and to have S be negative and $\approx -\frac{1}{2}$). It is known that for weak coupling, the scattering parameter S is temperature-dependent and is about $-\frac{1}{2}$ for $\theta/T \sim 2.5$ ^{20,21} ($\approx 225^\circ\text{K}$ in CdF_2). If this is true for intermediate coupling also, it is conceivable that polar scattering alone limits the mobility. But this remains to be seen and awaits a modification of Langreth's theory. In the event of such an uncertainty, we assign the value of $S \approx -\frac{1}{2}$ to the other known possible scattering mechanisms, which might provide a better fit to the experimental mobility, in conjunction with the scattering due to polar optical modes.

b. Acoustic Mode Scattering

Possible mechanisms with a value of $S \approx -\frac{1}{2}$ could be acoustic mode scattering¹⁸ or space charge scattering.²² Space charge scattering²² will depend on the presence of defects and dislocations. We have looked at the dislocation density and found that, at room temperature, it is of the order of $10^5/\text{cm}^2$. This density is not sufficiently large to affect the mobility drastically. It is difficult to calculate the mobility due to scattering by acoustic modes since we do not know the value of u_i , the sound velocity, or that of E_{1c} , the deformation potential, in the expression for μ for this mechanism:

$$\mu_{\text{acc}} = \frac{1}{3} (8\pi)^{1/2} \frac{e\hbar^4 d u_i^2}{(kT)^{3/2} m^{*5/2} (E_{1c})^2}, \quad (11)$$

where d the density of the material = 6.4 g/cm^3 for CdF_2 . We can, however, calculate μ_{acc} in such a way that

$$\mu_{\text{exp}}^{-1} = \mu_p^{-1} + \mu_{\text{acc}}^{-1} \quad (12)$$

at higher temperatures. The validity of such a calculation is, in fact, limited. With the value of μ_{acc} thus calculated, we can determine the value of the parameter (u_i/E_{1c}). In order to determine the value of u_i , we plotted sound velocity versus density for CaF_2 , BaF_2 , and SrF_2 , which have the same crystal structure as CdF_2 . By extrapolating this plot to the density corresponding to CdF_2 , we obtain $u_i \cong 2 \times 10^5 \text{ cm/sec}$. Using this value, we get $E_{1c} \cong 8.2 \pm 1 \text{ eV}$. This value is reasonable when compared with the value of E_{1c} of

other ionic crystals.²³ These two mechanisms account for the experimental mobility down to approximately 250°K (see Fig. 6).

c. Ionized Impurity Scattering

At temperatures lower than 250°K , ionized impurity scattering may be the additional scattering mechanism. The Brooks-Herring treatment¹⁴ gives the mobility due to ionized impurity scattering by the expression

$$\mu_I = \frac{2^{7/2} (kT)^{3/2} \epsilon_0^2}{\pi^{3/2} e^3 m^{*1/2} (n + 2N_A)} \times \{ \ln [6m^* (kT)^2 \epsilon_0 / \pi e^2 \hbar^2 n] \}^{-1}, \quad (13)$$

where $N_A = N_D - n_0$ (see Table V); all other symbols have their usual meaning. A composite result due to the three mechanisms, calculated by using the expression

$$\mu_{\text{Tot}}^{-1} = \mu_p^{-1} + \mu_{\text{acc}}^{-1} + \mu_I^{-1}, \quad (14)$$

is shown in Fig. 6. For sample 8, the calculated value of mobility due to ionized impurity scattering alone seems to be in good agreement with the experimental mobility in the temperature region $150\text{--}300^\circ\text{K}$. For sample 9, the agreement between calculated μ_I and the experimental mobility is good throughout the entire temperature region plotted. For samples 10 and 11, which are lightly doped, μ_I is combined with μ_p and μ_{acc} . Calculated for sample 10, μ_{Tot} is in very good agreement with the measured mobility, but for sample 11, a discrepancy of up to 30% between μ_{Tot} calculated and the measured mobility is noted. In general, the agreement between the calculated and the experimental μ is good. We have also included the mobility data of a CdF_2 : 0.01% Yb sample, annealed at 500°C , from Prener and Woodbury⁷ to show that the mobility of their sample behaves similarly to ours. A sharp decrease in experimental mobility at lower temperatures in all samples is caused by impurity-banding effects.

V. CONCLUSIONS

We have investigated experimentally the resistivity, Hall coefficient, and mobility of a large number of samples of semiconducting CdF_2 doped with varying amounts of yttrium over the temperature range $425\text{--}4.2^\circ\text{K}$.

We conclude that semiconducting CdF_2 :Y exhibits impurity-band conduction. This behavior can be characterized with the activation energies ϵ_1 , ϵ_2 , and ϵ_3 , as has been done in other semiconductors. We assume the hydrogenic nature of the Y donor to interpret our results. We can seemingly resolve the discrepancy which exists between the calculated and the observed activation energy and characterize the impurity banding if the static dielectric constant and the m_c , the bare

²⁰ D. J. Howarth and E. H. Sondheimer, Proc. Roy. Soc. (London) **219**, 53 (1953).

²¹ S. S. Devlin, in *Physics and Chemistry of II-VI Compounds*, edited by M. Aven and J. S. Prener (North-Holland Publishing Co., Amsterdam, 1967), Chap. 11.

²² L. R. Weissberg, J. Appl. Phys. **33**, 1817 (1962).

²³ H. Kawamura, J. Phys. Chem. Solids **5**, 256 (1958).

conduction mass, are used to calculate a^* and ϵ_i . This, however, neglects any polaron effects. This is not understandable since the material is highly polar with a coupling constant $\alpha \approx 3.3$. The lack of good agreement between theory and experiment suggests that the simple semiconductor theories do not adequately describe the donor states in a polar material. The experimental Hall mobility can be fitted over a wide range of temperatures by assuming a combination of various scattering mechanisms. The polar optical mode and the acoustic mode, together, provide the fit down to 250°K. Below this temperature, ionized impurity scattering seems to be the additional mechanism.

ACKNOWLEDGMENTS

We are grateful to Dr. F. Trautweiler and his group for growing the CdF_2 crystals used in this investigation. We should like to thank Dr. D. Matz, Dr. F. Trautweiler, and F. Moser for helpful discussions during the course of this work. The valuable comments by Dr. D. C. Hoesterey on the manuscript are gratefully appreciated. We are grateful to W. Pinch and W. Selke for their technical assistance. We acknowledge the help of R. Ambrose in the atomic absorption analysis of our samples. We are thankful to Dr. D. L. Losee for evaporating titanium-gold contacts on glass plates.

Dielectric Screening of the Electron-Hole Interaction in Small-Gap Semiconductors

JÜRGEN K. KÜBLER*

Department of Physics, Texas A&M University, College Station, Texas 77843

(Received 29 January 1969)

The dielectric function that screens the electron-hole interaction in semiconductors has been derived from first principles, and is found to differ in an essential way from the usual random-phase-approximation (RPA) dielectric function. This screening function determines the binding energy of the exciton, and hence it is important for the theory of the excitonic insulator. We have studied the binding energy of the exciton for a simple band structure, and find that the case considered does not become unstable toward exciton formation, whereas the usual dielectric function in RPA predicts the excitonic instability.

I. INTRODUCTION

THE semiconductor-semimetal phase transition with a possible intermediate excitonic insulator phase has recently received considerable attention in connection with substances where the energy gap can be changed.^{1,2} The ideas developed for the excitonic insulator have subsequently been used to describe the Mott transition in heavily doped semiconductors.^{3,4} The possibility of the excitonic insulator phase is based on the assumption that the binding energy of the exciton, E_B , remains nonzero for vanishing energy gaps and certain band structures. The binding energy E_B is, apart from some constants, given by ϵ_0^{-2} , where ϵ_0 is some dielectric screening constant. Thus one explains why ϵ_0 remains finite for vanishing gaps.⁵ In situations where the energy gap G is smaller or equal to the binding energy E_B , the normal ground state of the semiconduc-

tor becomes unstable toward exciton formation and the new ground state has many interesting properties.^{1,2} Even though it is clear that the strong electron-hole interaction ($\epsilon_0 < \infty$) is at the heart of the theory, the nature of the screening function has never been explored sufficiently, at least not to our knowledge. Haken's theory^{6,7} seems inapplicable to small energy gaps, and the whole problem still seems to be as summarized by Knox⁸ in 1963. From Kohn's theory⁹ of the interaction of an electron with a test charge or with an impurity, it is plausible that the usual dielectric function in the random-phase approximation (RPA)¹⁰ screens the electron-hole interaction. In this paper we investigate this assumption and find that it is not really justified. In Sec. II A we formulate the screening function using many-body techniques.¹¹ In Sec. II B we show how our formulation gives the usual dielectric function

* Present address: Abteilung für Physik, Ruhruniversität, Bochum, Germany.

¹ D. Jérôme, T. M. Rice, and W. Kohn, *Phys. Rev.* **158**, 462 (1967).

² B. I. Halperin and T. M. Rice, in *Solid State Physics*, edited by F. Seitz, D. Turnbull, and H. Ehrenreich (Academic Press Inc., New York, 1968), Vol. 21.

³ W. Kohn, *Phys. Rev. Letters* **19**, 789 (1967).

⁴ N. F. Mott and E. A. Davis, *Phil. Mag.* **17**, 1269 (1968).

⁵ J. des Cloizeaux, *J. Phys. Chem. Solids* **26**, 259 (1965).

⁶ H. Haken, *Fortschr. Physik* **6**, 271 (1958).

⁷ H. Haken and W. Schottky, *Z. Physik. Chem. (Frankfurt)* **16**, 218 (1958).

⁸ R. S. Knox, *Solid State Phys. Suppl.* **5**, 78 (1963).

⁹ W. Kohn, *Phys. Rev.* **105**, 509 (1957); **110**, 857 (1958).

¹⁰ D. Pines, *Elementary Excitations in Solids* (W. A. Benjamin, Inc., New York, 1963). Almost all relevant references can be found here.

¹¹ A. A. Abrikosov, L. P. Gorkov, and I. E. Dzyaloshinski, *Methods of Quantum Field Theory in Statistical Physics* (Prentice-Hall, Inc., Englewood Cliffs, N. J., 1963).